The EMC of Orbital Angular Momentum (OAM) Based Wireless Communication

Michael Wulff, Graduate Student Member IEEE, Lei Wang, Senior Member IEEE, and Christian Schuster, Senior Member IEEE,

Abstract—In recent years, the interest in the usage of orbital angular momentum (OAM) modes in wireless communication increased and the corresponding research on the integration of OAM modes into modern communication systems has started. OAM promises to increase the data rate by using the modes as multiple independent communication channels. The fields of the different OAM modes are characterized by their spiral phase pattern, which differs from that of plane waves. OAM modes used in wireless communication are orthogonal, meaning they can be excited and received independently in certain environments, which promises better utilization of the spatial dimension. However, OAM-based communication is shown to be strongly susceptible to interference, refection and symmetry disruptions, requiring knowledge in and a careful consideration of the EMC of these systems. In this context, this contribution discusses the differences between OAM modes and conventional antennas and waves in classical EMC issues such as shielding and interference and highlights the crosstalk between OAM modes resulting from geometric asymmetries. To appropriately design an OAM-based communication and solve its EMC problems, the main lessons learned are summarized and their practical implications are discussed.

Index Terms—Aperture penetration, interference, orbital angular momentum (OAM), shielding.

I. Introduction

Wireless communication up to the THz radio frequency (RF) range is more important than ever in modern times, as the number of devices that communicate continues to grow and devices such as smartphones require ever higher data rates. For this reason, the technical standard of wireless communication, such as the fifth-generation standard (5G), is constantly being improved. Moreover, research on the sixth-generation (6G) standard [1], [2] has started, utilizing frequencies up to 10 THz. In general, data is transmitted using resources in time, frequency, polarization, and space. To increase the data rate, commonly new frequency resources are utilized, creating new challenges for RF components. However, to meet the demand for high data rates, it is advisable to also make more efficient use of the other dimensions, such as space. In modern communications, multiple input multiple output (MIMO) antennas are used to create multiple beams in space to transmit separate data streams, thus utilizing the spatial dimension. One promising method to use the spatial dimension more efficiently is to utilize OAM modes, as discussed in [3] from a communication perspective. OAM modes were first investigated in optics and only later in RF antenna communication [4]. They differ from the commonly used plane waves through their spiral field distribution, as depicted in Fig. 1. These OAM modes can be excited with an array of circularly arranged elements, as shown in Fig. 1 using the example of circular patch antennas. To excite a certain mode, the array elements are excited with a linearly increasing phase, resulting in a field with the same phase distribution, which in turn manifests itself in the spiral field distribution in Fig. 1. There are multiple OAM modes, which differ in their spatial phase distribution, as illustrated in Fig. 2. In certain environments, they are orthogonal in space, i.e., each mode can be excited and received separately, and no mode can arise as a superposition of the other modes. For wireless communication, this opens the possibility to use the OAM modes as separate parallel communication channels. For this reason, there is increasing interest in the research of OAM modes in the RF domain [5], [6], despite challenges such as beam misalignment and beam divergences [7].

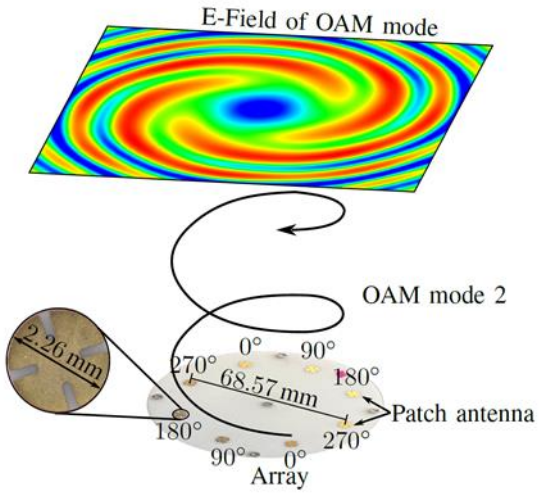

Fig. 1. OAM mode excited by a patch antenna array. The phase distribution on the array and the field plot belong to OAM mode 2. The array was manufactured in [8].

As shown by Fig. 2, all OAM modes (except OAM mode 0) differ from plane waves by their phase distribution in space. While the phase of a plane wave is constant on the planar wavefront, see Fig. 2 (a), in OAM waves the planes of constant phase form a helical surface. These differences raise the question of how the behavior of OAM waves differs from plane waves and what impact this has on traditional EMC issues of wireless communications involving OAM waves. When OAM modes are introduced into modern communication systems the resulting EMC problems need to be addressed. As far as the

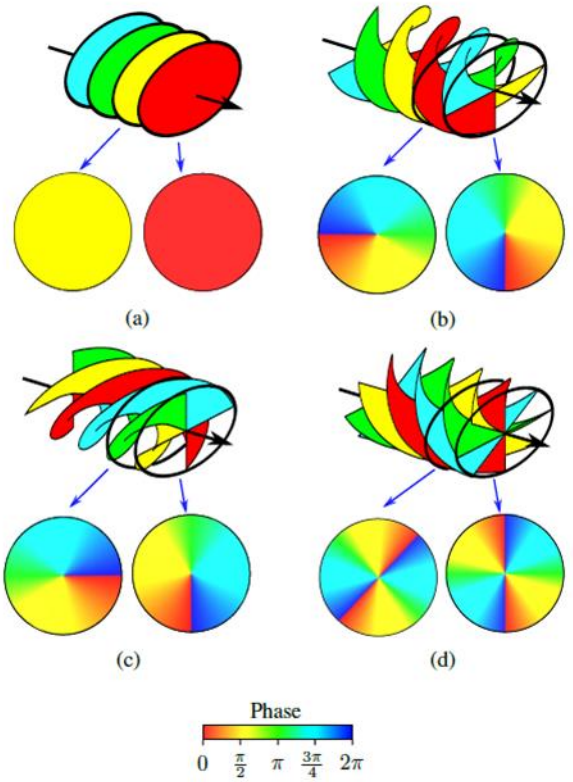

Fig. 2. Phase distribution of OAM mode 0 (and a plane wave) (a), OAM mode 1 (b), OAM mode -1 (c) and OAM mode 2 (a). A 3D illustration and two wavefronts are shown for every mode. The black arrow indicates the propagation direction.

authors are aware, these EMC perspectives of the OAM modes have so far only been examined in detail by the authors. This article introduces OAM-based RF communication, its core issues, and previous research efforts. Subsequently, this article aims to discuss the difference in interference, refection and shielding of OAM waves as they were identified as most relevant in the context of wireless communication, and especially the susceptibility of higher OAM modes has been found to be an issue. Moreover, the presence of multiple modes introduces the question of the relevance of crosstalk between the OAM modes introduced by certain environments.

II. OAM Modes in Wireless Communication

A. Utilization and Properties

In this article uniform circular arrays (UCAs) are discussed, as they can excite and receive multiple modes in parallel. In these arrays, the individual antennas are arranged in a circle with uniform angular spacing, as shown in Fig. 3. To excite an OAM mode, the array elements are fed with a signal of the same amplitude and a phase that is equivalent to the phase of the desired OAM mode. Fig. 3 (a) and (b) show the phases applied to excite OAM mode 1 and 2 respectively. The phase distribution indicated in the background shows the phase distribution of the desired OAM modes. In general, the array

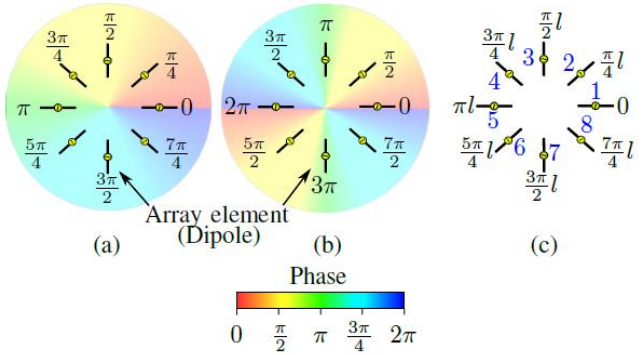

Fig. 3. Phase excitation of a UCA for OAM mode 1 (a), OAM mode 2 (b) and OAM mode l. The array elements are numbered in blue.

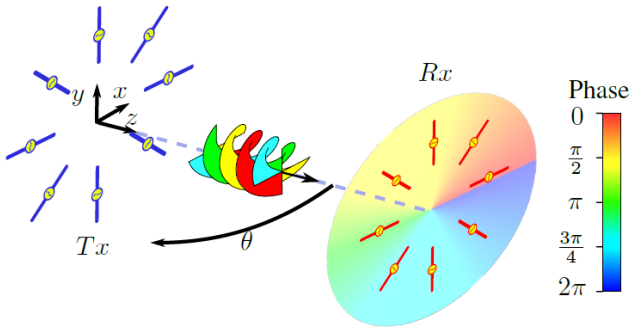

Fig. 4. The communication between two aligned UCAs. The phase received by Rx is indicated for the aligned case.

elements of an N element UCA have to be excited using the port voltage

$$v_n = \frac{v_0}{\sqrt{N}} \exp\left(\frac{2\pi}{N} \cdot l \cdot n\right) \quad (1)$$

to excite an OAM mode with the mode number l. Here v_0 is the complex amplitude of the OAM mode and n is the element number. For a UCA with $N = 8$ elements Fig. 3 (c) shows the corresponding phases for OAM mode l. An array with N elements can excite N different modes. In case of $N = 8$, these are$l = \{0,1,-1,2,-2,3,-3,\pm 4\}$. The last mode is a combination of $l = 4$ and $l = -4$, since using Eq. (1) both lead to a phase difference between adjacent elements of π, so they cannot be distinguished.

For the utilization of OAM modes in a communication scenario the respective orientation of the UCAs is important to consider. When two UCAs communicate, they have to be aligned as shown in Fig. 4. Only in this configuration, the incident OAM wave hits the receiving array (Rx) with the same phase distribution used for mode excitation. Tilting the Rx array or shifting it in the x or y direction alters the received phase pattern and prevents the Rx array from being able to uniquely distinguish between OAM modes, disrupting the orthogonality of the modes. This problem is addressed by either ensuring beam alignment or by compensating for the misalignment in the wave excitation or reception using beam steering [7]. The

Method	Type	OAM modes	Working Frequency	System Complexity	Received Wavefront	Ref.	Year
Spiral Phase Plate	Excitation / Reception	Single	Single	Low	Full	[9]	2014
Spiral Reflector	Excitation / Reception	Single	Single	Low	Full	[10]	2012
Traveling Wave Antenna	Excitation	Single	Single	Low	-	[11]	2015
Metasurfaces	Excitation	A Few	Single	Low	-	[12]	2023
Uniform Circular Array (UCA)	Excitation / Reception	Multiple	Not Limited	High	Full	[13]	2017
Single Point Estimation	Excitation	Single	Not Limited	High	One Point	[14]	2010
Phase Gradient Method	Excitation	Single	Not Limited	Low	Two Points	[14]	2010
Partial Aperture Sampling Method	Excitation	Multiple*	Not Limited	High	Partial	[15]	2016

TABLE 1. Overview of methods for the excitation and reception of OAM Modes. *Only some modes are orthogonal.

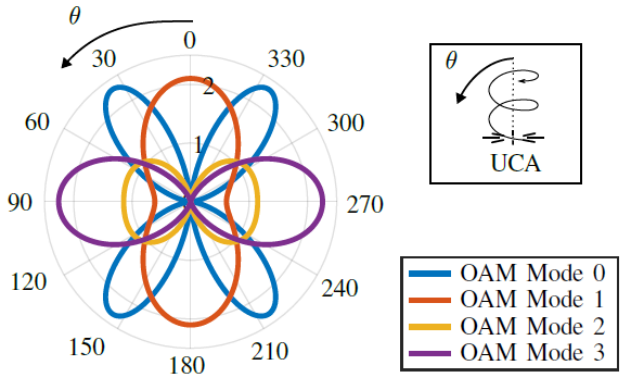

Fig. 5. Directivity of a UCA with radial dipole antennas. The 2D radiation pattern is evaluated along θ as indicated on the top right.

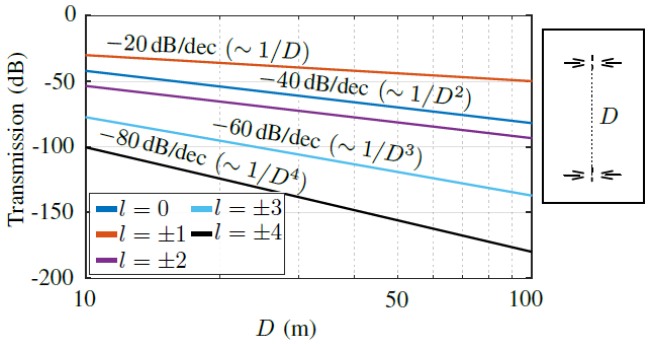

Fig. 6. Transmission between two UCAs in free space over the distance D. The slope of the transmission is indicated above the curves.

preservation of the phase pattern is one of the main concerns when it comes to the prevention of crosstalk between modes.

Equally important for the utilization of OAM waves is the beam divergence. The field of most OAM modes contains a field singularity where the field magnitude weakens towards the center of the beam. They occur when fields of the same direction but different phases converge at one point. The OAM modes that do not form a field singularity in the beam center depend on the orientation of the elements of the UCA, as determined by [21]. For the UCA with radial elements used in this article, these modes are OAM modes 1 and -1. Fig. 5 shows the radiation pattern of the different OAM modes using the UCA with radial elements. The fact that the OAM mode 0 generates a field singularity even though it has a uniform phase, as shown in Fig. 2 is due to the fact that the UCA with radial elements imposes the phase on the spherical coordinates of the fields. Apart from that, it can be seen that the field magnitude around the beam center ($\theta = 0$) decreases with increasing mode number $l > 1$. Thus, the higher the mode number, the more the beam diverges. Current efforts to solve this problem include the use of a dielectric lens [22] or enlarging the array [23]. This property of OAM waves causes the mode transmission of higher OAM modes to decrease with higher powers of $1/D$, see Fig. 6, which in turn increases the susceptibility of higher modes to noise or interference, as will be explained in the next section.

B. Overview of Research Status

In the RF domain, the majority of research on OAM has focused on the excitation and reception of OAM modes and experimental demonstrations of applications of OAM modes. This section provides a brief overview of research in these areas. TABLE 1lists some of the common excitation and reception methods, which differ in their complexity and their ability to use multiple modes or frequencies. To convert a plane wave into an OAM mode, the spiral phase plate uses a dielectric plate and the spiral reflector uses a metal reflector. The traveling wave antenna creates an OAM wave by radiating along a continuous structure. These three methods are not complex but have the disadvantage that they can only be used for a single mode and a single frequency. The metasurface converts a plane wave into an OAM mode by modifying its surface impedance using sub-wavelength structures. This method enables the excitation of several OAM modes if the incoming plane waves differ, for example, in their angle of incidence. The UCA allows the use of as many OAM modes as the array has elements, but is more complex than the other methods. The usable frequencies are given by the array elements used. Because of this flexibility, UCAs are the preferred excitation method in most experiments. All the reception methods mentioned so far require the full wavefront

Application	Antenna Type	Frequency	Data Rate	Bandwidth	No. of Modes	Distance	Evaluation	Ref.	Year
Communication	Spiral Phase Plates	73.5 GHz	3 Gb/s	5 GHz	2	2 m	-	[16]	2017
Communication	UCAs	28 GHz	200 Gbit/s	1 GHz	5	10 m	-	[17]	2018
Communication	UCAs	40 GHz	117 Gbit/s	1.5 GHz	7	200 m	-	[6]	2021
Radar (Rotation)	UCA and Horn	1 GHz	-	-	1	0.5 m	-	[18]	2016
Radar (Resolution)	UCA	10 GHz	-	0.2 GHz	41	50 m	FFT	[19]	2022
Radar (Resolution)	UCA	9.9 GHz	-	0.2 GHz	2	8 m	Sparse Bayesian Learning	[20]	2017

TABLE 2. Overview over experimental demonstrations of OAM applications.

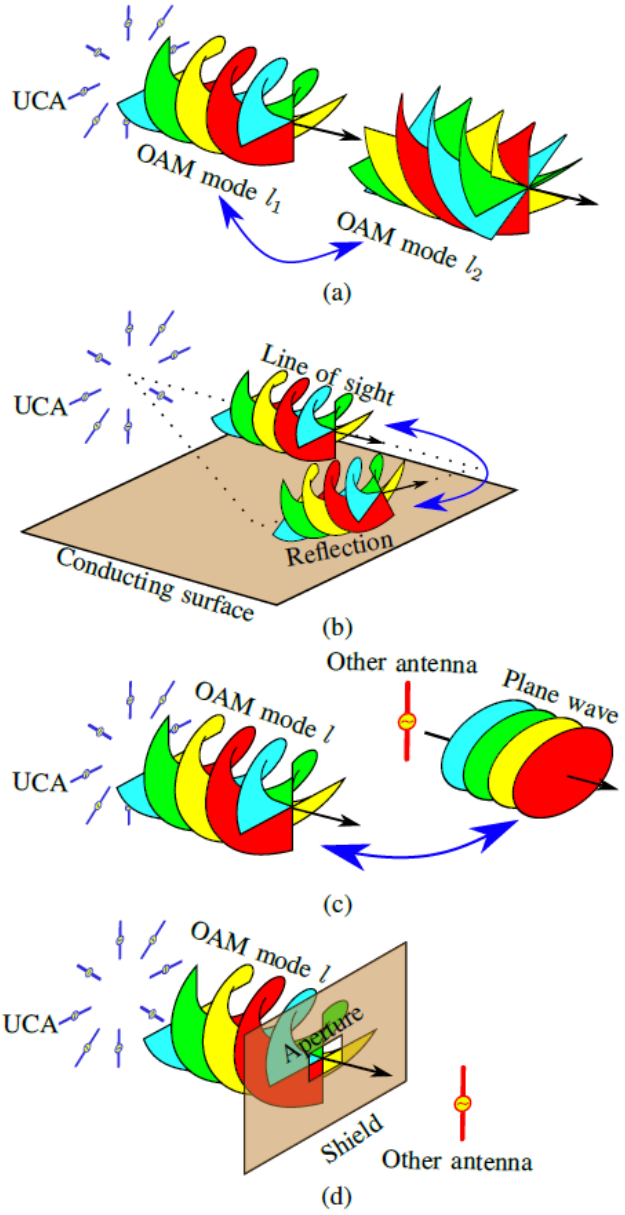

Fig. 7. Three EMC issues of OAM modes. (a) is the crosstalk within an OAM mode system, (b) is the reflection of an OAM mode, (c) is the interference between an OAM mode system and other antennas, and (d) is the aperture penetration of OAM modes.

of an OAM mode, i.e. the entire phase variation around the field singularity. The obvious downside of this is the receiver has to be placed in the field singularity. Alternative methods to receive an OAM mode are the single point estimation, the phase gradient method, and the partial aperture sampling method. Here, a varying number of points is used on only part of the wavesfront to detect the OAM modes. These approaches reduce the size of the receiver and allows its placement further from the field singularity, but also the number of modes that can be used in parallel.

The two most important applications for OAM modes currently being researched are communication and radar, see TABLE 2. For communication applications, there are many experimental demonstrations, three of which are listed in Table TABLE 2. For example, [6] achieved a data rate of 117 Gbit/s over a 200 m wireless link, showing the potential OAM modes can provide in the communication domain. In the radar domain, efforts are being made to detect the rotation of objects with the aid of OAM modes and to improve the resolution of the target cross-section.

III. EMC Issues of OAM Modes

The OAM modes radiated by a UCA form a mode system that can interact with itself, the environment, or other antennas. The potential EMC challenges of a system radiating electromagnetic (EM) waves in are well understood, and thus the key question is of the differences between OAM waves and conventional sources such as plane waves or simple antennas. For which issues is the behavior comparable and requires no additional measures, and which issues are different and require special consideration? For OAM modes, four aspects were identified as most important for wireless communication. The first is crosstalk within the mode system, seen in Fig. 7 (a). This can be a result of the environment. With the aim of using the orthogonality of the OAM modes, the crosstalk must be mitigated as much as possible. The second is the reflection of OAM modes, see Fig. 7 (b). These create multi-path propagation issues that can disrupt data transmission. As UCAs are not used in the direction of strongest transmission to preserve the mode orthogonality, reflections need to be considered. The third is the interaction between an OAM mode system and another antenna system, seen in Fig. 7 (c). Unintended interactions or interference may occur either with

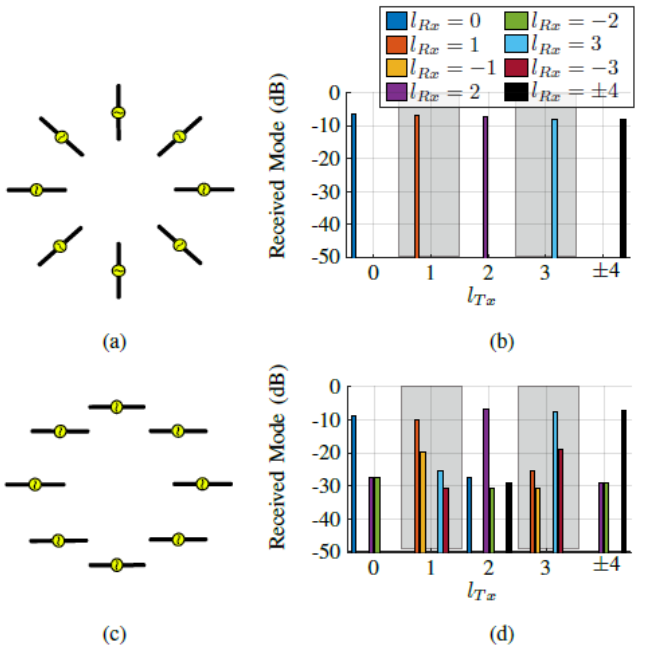

Fig. 8. Array with (a) radially and (c) horizontally arranged elements. Reflected modes (l_{Rx}) when only one mode is transmitted (l_{Tx}) by the unmatched array with (b) radially and (d) horizontally arranged elements.

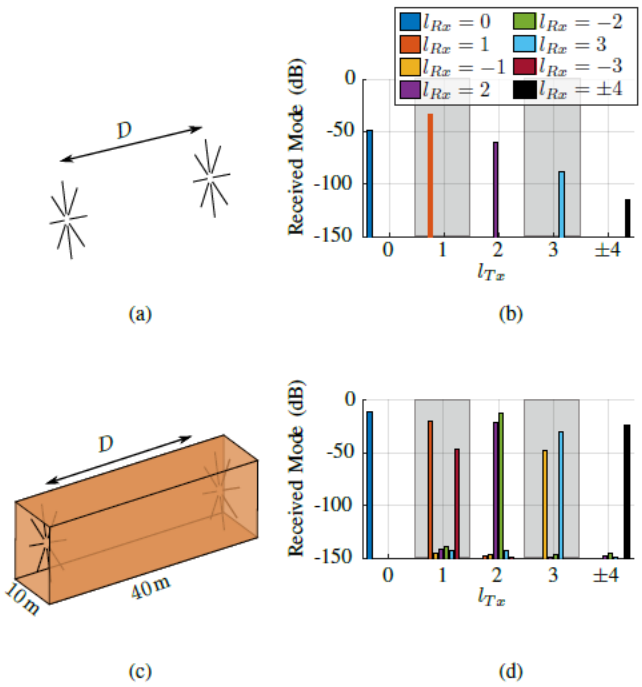

Fig. 9. Communication setup in (a) free space and (c) a square corridor. Received modes (l_{Rx}) when only one mode is transmitted (l_{Tx}) in the (b) free space and (d) square corridor setup. $D = 30$ m is used. Figure adapted from [27] © 2023 IEEE.

the OAM modes interfered by the other antenna or vice versa. Interference is generally to be avoided, but it may be unavoidable in crowded environments. Thus, knowing the effects of interference and adapting to it is essential for communication scenarios. The last aspect is the shielding and aperture penetration of OAM modes, seen in Fig. 7 (d). As shielding is essential for the proper function of some devices, it is impotent to assess how well OAM modes can be shielded.

A. Crosstalk Within the OAM Mode System

As the OAM mode system transmitted by a UCA with N elements can contain up to N modes, the question of crosstalk between these modes arises similarly to the crosstalk between common mode and differential mode on transmission lines. And like the common mode and differential mode on balanced lines, the OAM modes use spatially orthogonality. For both systems, the perturbation of the spatial symmetry can lead to crosstalk between the modes. In fact, the OAM mode system can be viewed as an extension of the common mode and differential mode system to N conductors or antennas [24], [25]. It was found that the array and the environment of the communication must be cyclic symmetric to ensure OAM mode orthogonality [26], [27]. In practice, this means that the array and the environment must 'look the same' in terms of S-parameter from every antenna port. Deviations from this introduce crosstalk between modes.

To illustrate the implications for the UCAs and the environment, we will look at examples of both. Starting with the UCA, the symmetry can be perturbed by, for example, changing the orientation of the array elements [21], [28] or modifying the array shape [26]. Fig. 8 illustrates the effect of changing the orientation of the array elements. The arrays shown consist of half-wave dipoles and are placed in free space. The frequency is 100 MHz, and the UCA radius measured from the dipole centers is 1 m. Fig. 8 (b) and (d) show the OAM modes reflected back into the ports (l_{Rx}) if only one mode (l_{Tx}) is excites. If $l_{Tx} = l_{Rx}$, this is a mode refection, if $l_{Tx} \neq l_{Rx}$, this is near-end crosstalk (NEXT). Mode with negative l_{Tx} behave analogously to their positive counterpart and are therefore not shown. For the array with radially arranged elements (a)-(b) the modes are reflected, but there is no NEXT. This array is cyclic symmetric as the array 'looks the same' from every port. In the array with horizontally arranged elements (c)-(d), the modes are reflected and there is NEXT between certain modes. This array is not cyclic symmetric.

For the environment, there are many ways to perturb the symmetry as shown in [27]. In Fig. 9 the comparison between a free space communication (a) and a communication in a square corridor (b) are shown. The array dimensions and the frequency are unchanged from the last example. Here, (b) and (d) show the OAM modes received by one array (l_{Rx}) if the other array transmits only one mode (l_{Tx}). If $l_{Tx} = l_{Rx}$, this is a mode transmission, if $l_{Tx} \neq l_{Rx}$, this is far-end crosstalk (FEXT). Mode with negative l_{Tx} behave analogously to their positive counterpart and are therefore not shown. In the free space case (a)-(b) no FEXT is detected as the environment is cyclic symmetric. In contrast, communication in the square corridor (c)-(d) gives rise to a strong FEXT between some

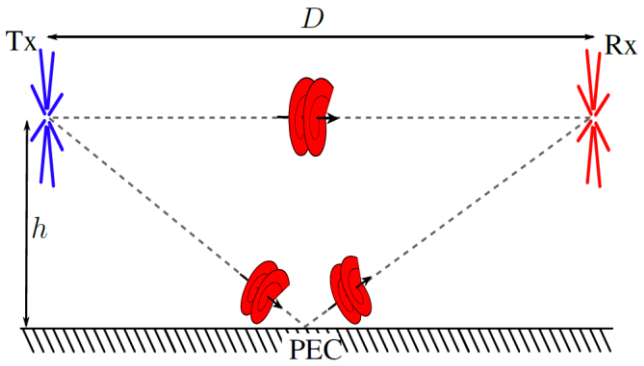

Fig. 10. Communication of two UCAs at a distance D and a height h about ground. Figure adapted from [30].

modes. This is not surprising, as the environment is not cyclic symmetric.

Both, [26] and [27] explored a method that allows the prediction of occurring crosstalk using the geometry of the array or environment, allowing the application of targeted geometric alteration to restore or partially restore OAM mode orthogonality. This method could be used to mitigate crosstalk. However, since it is usually not possible to influence the geometry, especially for the environment, this method may not be applicable in most scenarios. Alternatively, equalization can be used [29], which has the disadvantage of introducing overhead. Regardless, it is important to be aware of the effects of geometric changes on the OAM system when developing such a system.

B. Transmission over Conducting Ground

One of the most commonly encountered non-cyclic environments is the communication between two arrays above a conducting ground plane. Simultaneously, this scenario is a simple example of the reflection of OAM modes. In general reflections in the environment lead to multi-path propagation, which is usually addressed in software. However, the question of the difference in the susceptibility of OAM modes compared to classic antennas such as a dipole arises again.

To evaluate the effect of reflections for OAM modes, two UCAs are placed at a distance D at a height of 50 m about a conducting ground plane, as seen in Fig. 10. Here, half-wave dipoles are used. The frequency is 100 MHz, and the UCA radius measured from the dipole centers is 1 m.

Fig. 11 shows the mode transmission (Tr) and the arising crosstalk over D when either two dipoles communicate or two UCAs communicate using OAM mode 0, 1, or 2. The free-space transmission gives a comparison to assess the effect of the ground plane. In all cases, the ripples in the transmission indicate multi-path propagation, as the signals from multiple paths interfere constructively or destructively at different distances. However, the distance on which the ripple starts to show up varies. While they are noticed first for the dipoles and the strongest mode (1) at approximately the same distance,

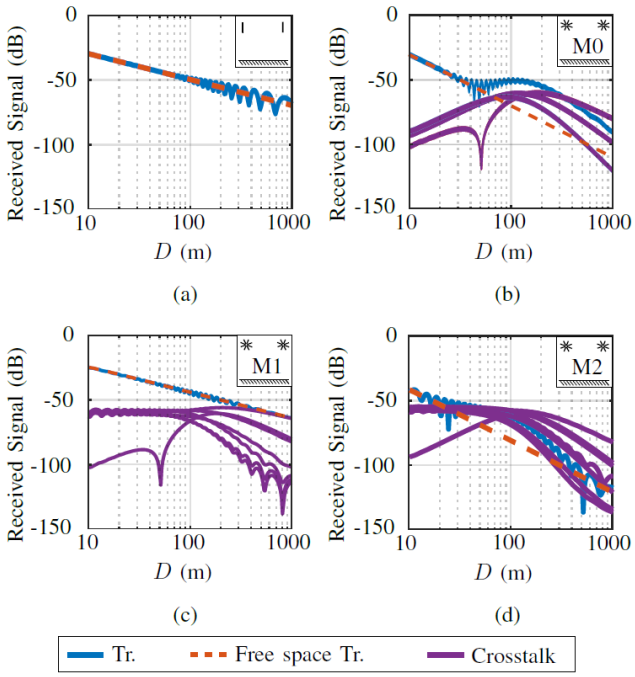

Fig. 11. Signals received by Rx when two dipoles (a) or two UCA communicate 50 m above ground using OAM mode 0 (b), OAM mode 1 (c), or OAM mode 2 (d). The sketch in the upper right corner of the plots indicates the setup and mode used.

multi-path effects occur at smaller distances for weaker modes. The problem here is that the reflection does not decay as fast as the direct transmission because it arrives from a different angle (see Fig. 5), so there are distance and mode combinations where the reflection is as strong or stronger than the direct transmission. The weaker the direct transmission, the smaller this distance. Moreover, the arising crosstalk overtakes the mode transmission at an increasingly smaller distance the weaker the OAM mode is.

Conclusively, all OAM modes that fall with a higher power of $1/D$ are especially susceptible to reflections and the multi-path propagation they create.

C. Interference of OAM Modes from a Third Antenna

The radiated interference of one system (victim) by another system (aggressor) is one of the commonly encountered EMC problems. In many cases, the victim is a printed circuit board or other component acting as an unintentional antenna. In other cases the antenna is intentional, but the received signal is undesired. These undesired signals either manifest as noise for the victim antenna and limit the achievable data rate or destroy the system. In our case, the Rx antenna trying to receive the OAM modes sent by Tx is the victim and some third antenna (Nx) sending non-destructive signals is the aggressor. Since the transmission of OAM modes with higher $|l|$ is known to decrease with higher powers of $1/r$ [21], the susceptibility of these modes to interference is of great concern.

The Nx antenna can be positioned anywhere in space, but

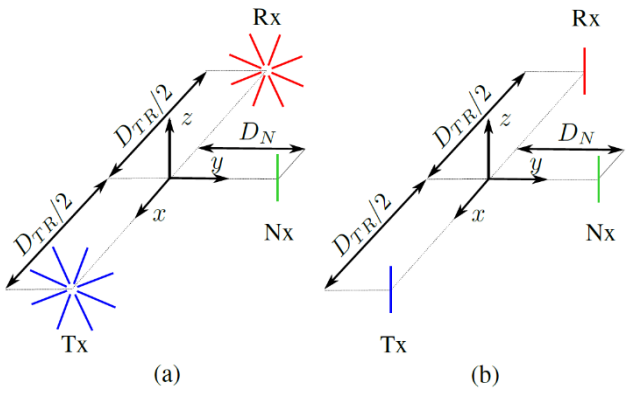

Fig. 12. Two communicating antennas, Tx and Rx, and an interfering antenna, Nx. In (a), UCAs are used, and in (b), single dipoles are used. Figure adapted from [30].

we found in [30], [31] that the setup shown in Fig. Fig. 12 (a) is sufficient to explore the differences in the susceptibility of OAM modes and other antennas. Here, a half-wave dipole is used as Nx, while Tx and Rx are UCAs consisting of radially arranged half-wave dipoles. The frequency is 100 MHz, and the UCA radius measured from the dipole centers is 1 m. The distance between Tx and Rx is D_{TR} and D_N is varied. To obtain a reference for the interference of non-OAM antennas, Tx and Rx are replaced by half-wave dipoles in a second scenario, see Fig. 12 (b).

With this setup, the effect of the interference should be demonstrated, but the introduction of the Nx antenna created additional disturbances. Here, three types of disturbances of the Tx-Rx communication are expected. The first is multi-path propagation, as the OAM modes are partially reflected by Nx. The second is crosstalk between modes, as the presence of Nx perturbs the symmetry of the environment and the third is the interference of Rx by the signal radiated by Nx.

In Fig. 13 the transmission (Tr) between Tx and Rx, as well as the crosstalk and interference are shown depending on D_N. To assess changes in the transmission, the free space transmission is included. In the case of crosstalk, only the strongest mode is displayed. All OAM modes and single dipoles are excited with the same power.

For the interference, the general behavior over D_N for the OAM modes and the dipole communication is the same, it falls with increasing D_N. The exception is that Nx does not interfere with some modes in certain positions, for example, for $D_N = 0$ only OAM modes 1 and -1 (not shown) are perturbed. The interference to the dipole Rx (a) is generally weaker than to the UCA Rx (b)-(f). This is mainly attributed to the different antenna sizes. The crosstalk behaves the same but is significantly weaker in this setup. While the interference does not differ significantly for the different modes, the transmission decreases significantly with increasing $|l|$ because of the field singularity mentioned before. This decreases the signal-to-noise ratio (SNR) for higher modes and shows a great susceptibility of these modes to interference. This effect occurs

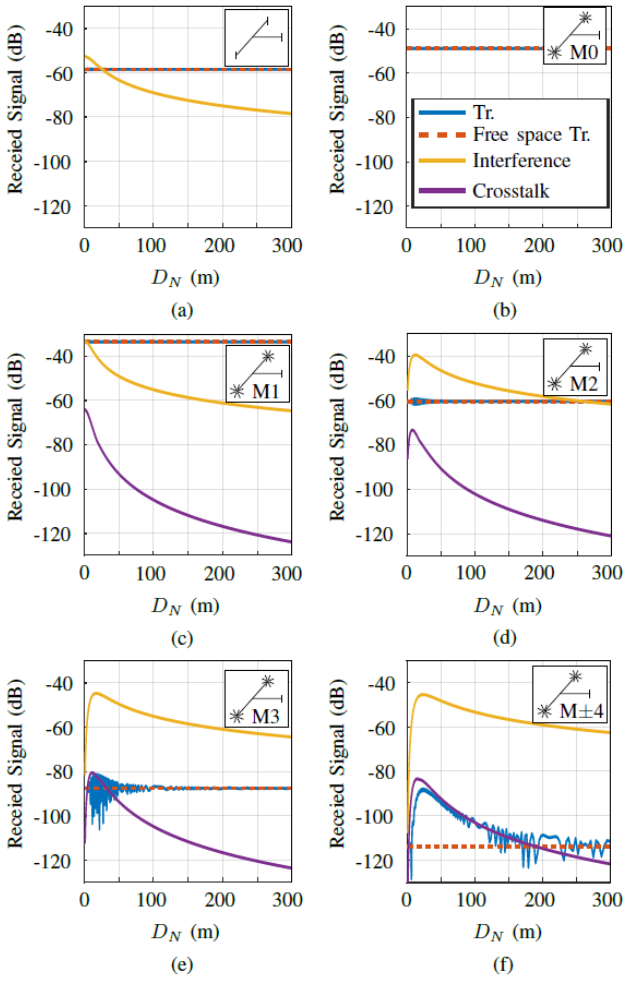

Fig. 13. Signals received by Rx when an interfering dipole Nx is placed at a distance D_N to the communication link, see Fig. 12. For (a), Tx and Rx are single dipoles. Otherwise, Tx and Rx are UCAs, transmitting using OAM mode 0 (b), 1 (c), 2 (d), 3 (e), or 4 (f). The sketch in the upper right corner of the plots indicates the setup and mode used. Figure adapted from [30].

because the OAM modes decay faster than the noise. A similar effect modifies mode transmission. As seen in Fig. 13 (d) - (e), the OAM transmission differs from the free space transmission, which is caused by multi-path propagation.

In conclusion, OAM modes with high mode number $|l|$ are increasingly susceptible to interference as the corresponding mode transmission decays faster than the interfering signal. The interference of classical antenna by an OAM mode shows no special effects and does not require additional consideration.

D. Aperture Penetration of OAM Modes

Shielding is a common method to protect a sensitive device from electric or magnetic fields. If deployed correctly, a shield can reduce the field that reaches the sensitive device by orders of magnitude. A shield can consist of various materials and can be designed to shield E-fields, H-fields, or EM waves. Here, the focus lies on a metal structure that shields EM waves. Since one needs to access the sensitive device or simply for

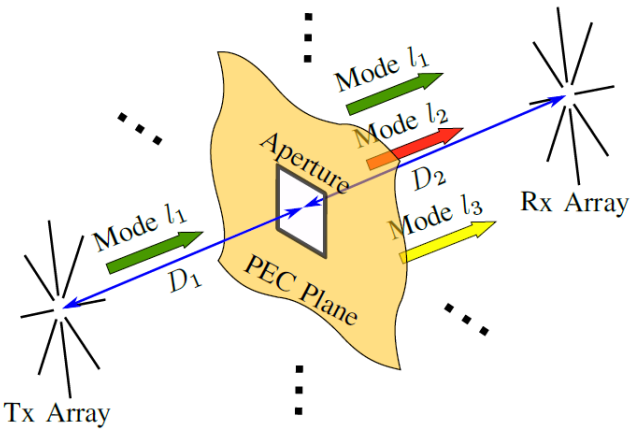

Fig. 14. Communication of two OAM array antennas through an aperture in an infinite PEC plane. A mode l_1 sent through an aperture can be converted to other modes, e.g. l_1, l_2, l_3. The Tx array and the aperture are placed $D_1 = 10\,\text{m}$ apart, and the Rx array and the aperture are placed $D_2 = 10\,\text{m}$ apart. Figure adapted from [32] © 2023 IEEE.

ventilation purposes, many shields have apertures. These apertures can be weak spots where the EM waves may enter the shield and, thus, the apertures need to be designed properly. Since the wavefront of OAM modes is quite complex, the question arises whether OAM modes can penetrate an aperture at all and whether the shielding of OAM modes differs from conventional EM wave sources.

First, the question of whether OAM modes can penetrate apertures at all is addressed, and if so, what happens to the orthogonality of the modes. To answer this question, an aperture is put onto an infinite PEC plane to study the effects of the aperture in isolation. Two UCAs try to communicate through the aperture, creating the setup shown in Fig. 14. The UCAs use radially arranged half-wave dipoles. The frequency is 100 MHz, and the UCA radius measured from the dipole centers is 1 m. For this investigation the simulation method and accuracy have been shown in [33] and the scenario itself has been evaluated in detail in [32]. In Fig. 15 the aperture penetration of the OAM modes is depicted for a square and circular aperture of varying sizes. The curves show the modes received by the Rx array when the Tx array transmits only OAM mode 0, 1, or 2. From the plots, one can conclude that OAM modes can penetrate apertures and that the mode penetration is mode selective and increases with aperture size. It is also noted that there is no crosstalk between OAM modes for the circular aperture, while there is crosstalk for the rectangular aperture. This can, as before, be attributed to the symmetry of the communication environment.

In order to answer how the shielding of OAM modes compares to the shielding of conventional sources, the aperture is now put on a PEC cavity, see Fig. 17 (a). As UCA, a monopole array is used to reduce the size of the arrays. The wires of the array have a length of 1.4 m, the array has a radius of 0.6 m, and the array plate has a radius of 0.9 m. As a comparison, the UCAs are replaced by monopole antennas (b)

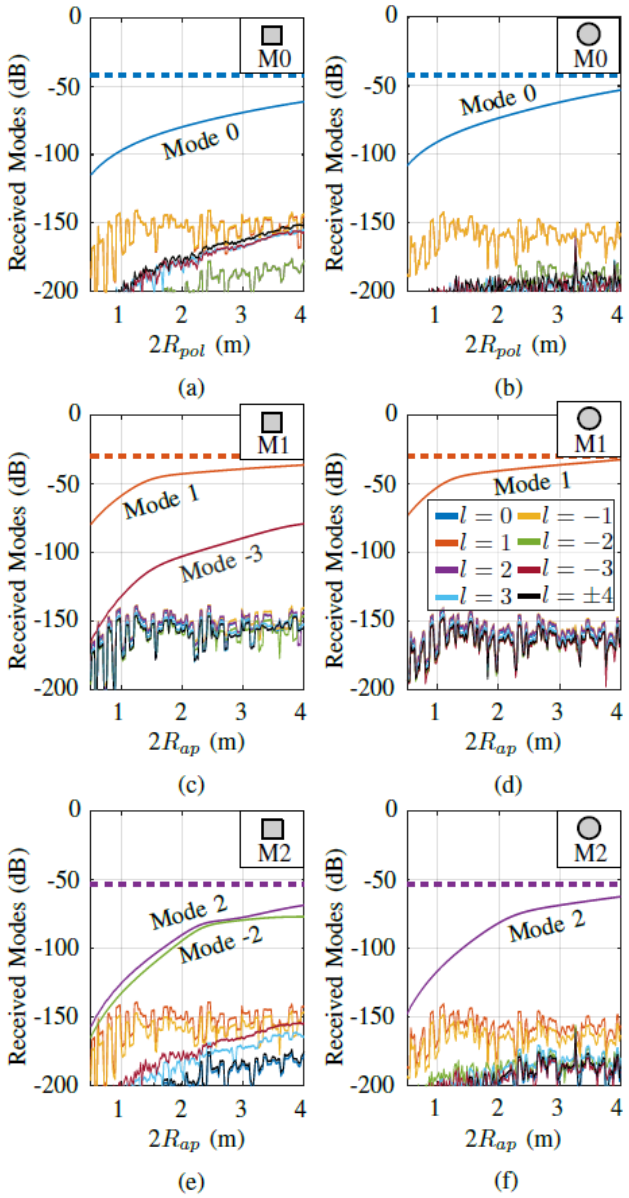

Fig. 15. Received modes (l) if mode 0 (a)(b), mode 1 (c)(d), mode 2 (e)(f) are transmitted. A square aperture with the diagonal $2R_{ap}$ (a)(c)(e) or a circular aperture with the diameter $2R_{ap}$ (b)(d)(f) is used. The received modes in free space (dashed lines) are given as a reference. The highly oscillating curves are due to numerical instabilities. Figure adapted from [32] © 2023 IEEE.

in the same orientation with the same wire length and a plate radius of 0.3 m. Further comparisons are made with incident plane waves propagating in the y direction and having an E-field in the x (c) or z direction (d). In this case, there are no antennas.

For a proper comparison the shielding effectiveness (SE) has to be defined for all three excitation methods. Generically the ratio of a quantity with and without a shield is evaluated. Here, the E-field in the center of the cavity is compared for the plane waves, the S-parameters using a reference impedance of 50 Ω are compared for the monopole antenna, and the mode transmissions are compared for the UCAs.

For this setup, Fig. 16 shows the SE over the frequency and

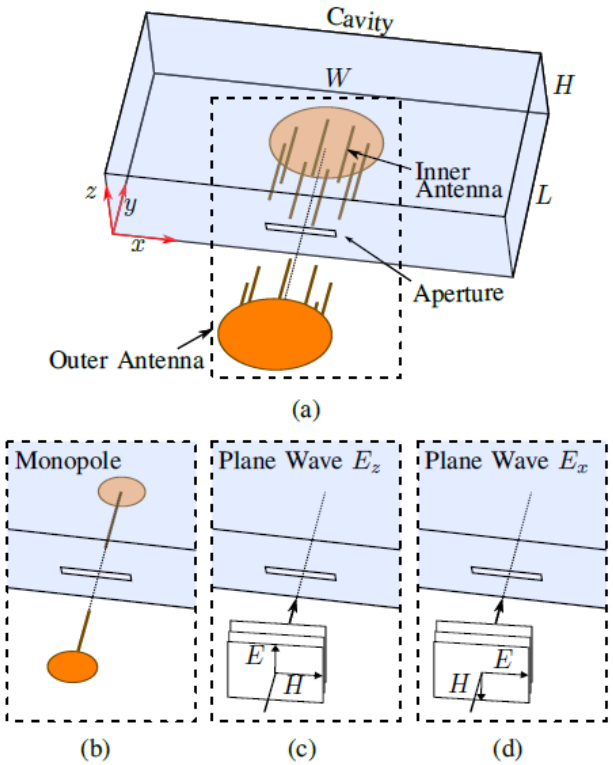

Fig. 17. Setup with a PEC cavity having the following dimensions: $W = 5.8$ m, $L = 3.5$ m, and $H = 2.5$ m. The cavity has an aperture on the front side. In (a) two UCAs, one inside and one outside antenna, are used. The inner antenna can be placed in the center of the cavity. Alternative excitations include monopoles (b) and plane waves (c)(d). Figure adapted from [34] © 2022 IEEE.

the largest structure size w for two different apertures. The apertures are a rectangular slot (a)(b), and a circular aperture (c)(d). Geometric dimensions of these apertures can be found in [34]. For the comparison of the three excitation methods, one has to keep in mind that the presence of the antennas modifies the resonances of the cavity. With this in mind, one can see that the SE of the OAM modes is never below the SE of the plane waves when no resonances are involved. Moreover, the SE is mode selective, similar to the aperture penetration. For the rectangular slots, OAM modes 1 and -1 (not shown) are shielded worse than the other modes and for the circular slot, OAM modes 2 and -2 (not shown) are shielded better than the other modes shown. Further comparisons, using more observation points, apertures, cavities, and antenna orientations can be found in [34].

All in all, it can be stated that the SE of the OAM modes behaves similarly to the SE of the other sources and that its magnitude is not significantly different either. So, from a shielding perspective, no additional considerations are required for OAM modes.

IV. Discussion and Conclusion

TABLE 3 compares the severity of EMC problems for OAM modes radiated by UCAs and single antennas. In summary,

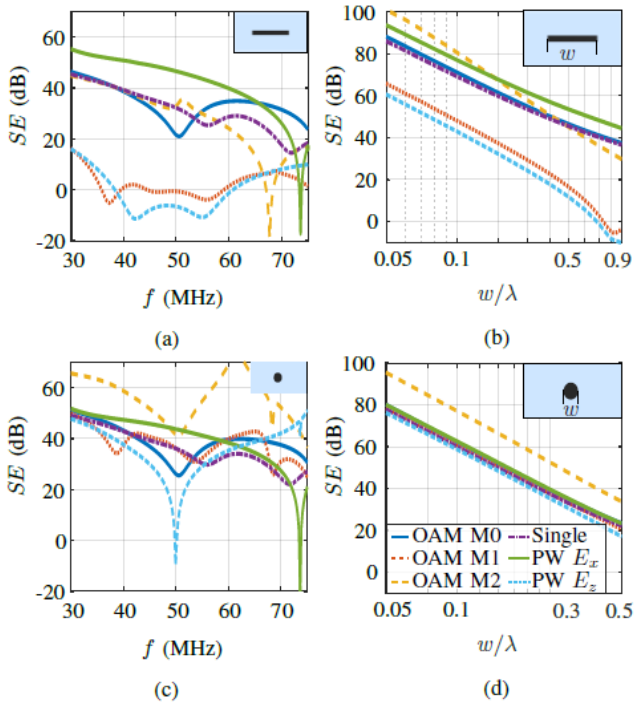

Fig. 16. Shielding effectiveness (SE) using different apertures over frequency (a)(c) and over the largest aperture dimension (b)(d) for OAM arrays, single monopole antennas (Single), and plane waves (PW). The corresponding aperture is displayed in the upper right corner of every plot. Figure adapted from [34] © 2022 IEEE.

	OAM modes	Single antennas	Additional action required?
Crosstalk between modes	non-cyclic environments.	-	Yes
Reflection	Higher modes very susceptible.	Moderately susceptible.	Yes
Interference	Higher modes very susceptible.	Moderately susceptible.	Yes
Shielding	Penetrates apertures depending on aperture shape and size.	Penetrates apertures depending on aperture shape and size.	Yes

TABLE 3. Comparison of the discussed EMC issues.

the EMC problems of radiated OAM modes in the RF domain that must be paid special attention to are susceptibility to perturbation of spatial symmetry, reflection, and interference of other antennas.

The perturbation of spatial symmetry manifests itself in an unsymmetrical communication environment or array geometry and leads to crosstalk between the different OAM modes. In practice one has little influence over the environment in most cases. However, where possible, such as in array design, it is recommended to influence symmetry to reduce crosstalk. Regarding unsymmetrical obstacles in the communication environment, one can reduce their importance for the communication link by focusing the OAM modes or reducing the distance between the arrays. Additionally, the communication system can implement an equalizer to mitigate

crosstalk or reduce the number of modes used if the SNR drops too far in the higher and weaker modes.

Reflections occur when the environment contains obstacles with reflective surfaces. Their severity depends on the environment and application. Weaker OAM modes with higher mode numbers are especially susceptible to the multi-path propagation created by reflections due to their fast decay over distance. The same recommendations stated above apply. Focusing the OAM modes or reducing the distance between the arrays may reduce the effect of reflections. Refrain from using higher OAM modes when their SNR gets too low or the multi-path effects become too strong.

The interference of other antennas is especially an issue for higher modes, for which the field decreases at a higher power of $1/D$. If possible the issue can be avoided by not using the USAs close to other antennas. Otherwise, the same recommendations stated above apply. If possible focus the OAM modes or reduce the distance between the arrays. Refrain from using higher OAM modes when their SNR gets too low.

All in all, the usage of OAM modes does require more consideration of the communication space, especially in crowded areas. The problems discussed probably cannot be avoided, but careful consideration of communications hardware and software can minimize them, allowing a better utilization of spatial dimensions.

Acknowledgment

This work was supported by the German Research Foundation (Deutsche Forschungsgemeinschaft, DFG) within the project 'Properties of Orbital Angular Momentum (OAM) Waves with Respect to Wireless Communication in Complex Environments and to Electromagnetic Interference' (WA 4543/1-1 and SCHU 2510/13-1).

Appendix

The authors would like to correct two mistakes from the paper [21]. First, the formula for the slope of the mode transmission of the arrays with tangential elements at the end of the first paragraph of the third section should be $-20 \cdot (1 + ||l| - |l_r||$ dB/dec. This error is repeated in the first paragraph of the fifth section. Second, in Table 1 of [21], the arrays with rotation numbers $l_r = \pm 1$ are incorrectly identified as arrays that cause a minor mode conversion. Instead, it should be the arrays with rotation numbers $l_r = 1$ and $l_r = -3$. Table 1 of [21] should be replaced with TABLE 4.

This error is repeated multiple times in the paper. Whenever $l_r = \pm 1$ is mentioned, it should be replaced with $l_r = 1$ and $l_r = -3$. This error can be found twice in the second paragraph of the third section, once in the third paragraph of the third section, once in the first paragraph of the fourth section, twice in the first paragraph of the fifth section, and once in the second paragraph of the fifth section. The authors regret these errors.

Type	normal	tangential	tangential		tangential		tangential		tangential
l \ l_r		0	1	-1	2	-2	3	-3	4
0	-40	-20	-40		-60		-80		-100
±1	-60	-40	-20		-40		-60		-80
±2	-80	-60	-40		-20		-40		-60
±3	-100	-80	-60		-40		-20		-40
0*	-120	-100	-80		-60		-40		-20
MMC	-135	-25	-110	-25	-25	-25	-25	-110	-25

TABLE 4. Slope of the OAM transmission in dB/dec as well as the maximum mode conversion (MMC) at $d = 100$ m for the different configurations.

Reference

[1] H. Tataria, M. Shafi, A. F. Molisch, M. Dohler, H. Sjöland, and F. Tufvesson, "6G Wireless Systems: Vision, Requirements, Challenges, Insights, and Opportunities," Proceedings of the IEEE, vol. 109, pp. 1166–1199, Jul. 2021.

[2] T. Nakamura, "5G Evolution and 6G," in 2020 IEEE Symposium on VLSI Technology, Honolulu, HI, USA, 2020.

[3] R. M. Henderson, "Let's Do the Twist!: Radiators, Experiments, and Techniques to Generate Twisted Waves at Radio Frequencies," IEEE Microwave Magazine, vol. 18, no. 4, pp. 88–96, 2017.

[4] B. Thide, H. Then, J. Sjöholm, K. Palmer, J. Bergman, T. D. Carozzi, Y. N. Istomin, N. H. Ibragimov, and R. Khamitova, "Utilization of Photon Orbital Angular Momentum in the Low-Frequency Radio Domain, "Phys. Rev. Lett., vol. 99, p. 087701, Aug. 2007.

[5] R. Chen, W.-X. Long, X. Wang, and L. Jiandong, "Multi-Mode OAM Radio Waves: Generation, Angle of Arrival Estimation and Reception With UCAs," IEEE Transactions on Wireless Communications, vol. 19, no. 10, pp. 6932–6947, 2020.

[6] Y. Yagi, H. Sasaki, T. Semoto, T. Kageyama, T. Yamada, J. Mashino, and D. Lee, "Field Experiment of 117 Gbit/s Wireless Transmission Using OAM Multiplexing at a Distance of 200 m on 40 GHz Band," in 2021 IEEE International Conference on Communications Workshops (ICC Workshops), Montreal, QC, Canada, 2021.

[7] Y. Zhang, W. Feng, and N. Ge, "On the Restriction of Utilizing Orbital Angular Momentum in Radio Communications," in 2013 8th International Conference on Communications and Networking in China (CHINACOM), pp. 271–275, Guilin, China, 2013.

[8] Z. Dong, Millimeter-Wave Stacked Patch Antenna For Wireless High Capacity Communication Using Orbital Angular Momentum (OAM). Bachelor's thesis, Heriot-Watt University (HWU), Edinburgh, UK, 2023.

[9] L. Cheng, W. Hong, and Z.-C. Hao, "Generation of Electromagnetic Waves with Arbitrary Orbital Angular Momentum Modes," Scientific Reports, vol. 4, pp. 2045–2322, Apr. 2014.

[10] F. Tamburini, E. Mari, A. Sponselli, B. Thid´e, A. Bianchini, and F. Romanato, "Encoding Many Channels on the Same Frequency Through Radio Vorticity: First Experimental Test," New Journal of Physics, vol. 14, p. 033001, Mar. 2012.

[11] S. Zheng, X. Hui, X. Jin, H. Chi, and X. Zhang, "Transmission Characteristics of a Twisted Radio Wave Based on Circular

Traveling-Wave Antenna," IEEE Transactions on Antennas and Propagation, vol. 63, pp. 1530–1536, Api. 2015.
[12] H. Yang, S. Zheng, H. Zhang, N. Li, D. Shen, T. He, Z. Yang, Z. Lyu, and X. Yu, "A THz-OAM Wireless Communication System Based on Transmissive Metasurface," IEEE Transactions on Antennas and Propagation, vol. 71, pp. 4194–4203, May 2023.
[13] C. Deng, K. Zhang, and Z. Feng, "Generating and Measuring Tunable Orbital Angular Momentum Radio Beams With Digital Control Method," IEEE Transactions on Antennas and Propagation, vol. 65, pp. 899–902, Feb. 2017.
[14] S. M. Mohammadi, L. K. S. Daldorff, K. Forozesh, B. Thide, J. E. S. Bergman, B. Isham, R. Karlsson, and T. D. Carozzi, "Orbital Angular Momentum in Radio: Measurement Methods," Radio Science, vol. 45, pp. 1–14, Aug. 2010.
[15] Y. Hu, S. Zheng, Z. Zhang, H. Chi, X. Jin, and X. Zhang, "Simulation of Orbital Angular Momentum Radio Communication Systems Based On Partial Aperture Sampling Receiving Scheme," IET Microwaves, Antennas & Propagation, vol. 10, pp. 1043–1047, Jul. 2016.
[16] H. Yao, H. Kumar, T. Ei, S. Sharma, R. Henderson, S. Ashrafi, D. Mac- Farlane, Z. Zhao, Y. Yan, and A. Willner, "Experimental demonstration of a dual-channel E-band communication link using commercial impulse radios with orbital angular momentum multiplexing," in 2017 IEEE Radio and Wireless Symposium (RWS), pp. 51–54, Phoenix, AZ, USA, 2017.
[17] Y. Yagi, H. Sasaki, T. Yamada, and D. Lee, "200 Gbit/s Wireless Transmission Using Dual-Polarized OAM-MIMO Multiplexing on 28 GHz Band," in 2019 IEEE Globecom Workshops (GC Wkshps), Waikoloa, HI, USA, 2019.
[18] M. Zhao, X. Gao, M. Xie, W. Zhai, W. Xu, S. Huang, and W. Gu, "Measurement of the Rotational Doppler Frequency Shift of a Spinning Object using a Radio Frequency Orbital Angular Momentum Beam," Opt. Lett., vol. 41, pp. 2549–2552, Jun. 2016.
[19] J. Liu, P. Wang, Q. Chen, M. Wan, and C. Zheng, "High-resolution detection of near-distance imaging with vortex electromagnetic waves," in 2022 3rd China International SAR Symposium (CISS), Shanghai, China, 2022.
[20] K. Liu, X. Li, Y. Gao, Y. Cheng, H. Wang, and Y. Qin, "High-Resolution Electromagnetic Vortex Imaging Based on Sparse Bayesian Learning," IEEE Sensors Journal, vol. 17, pp. 6918–6927, Sep. 2017.
[21] M. Wulff, L. Wang, C. Yang, and C. Schuster, "Effect of the Orientation of the Array Elements of Uniform Circular Antenna Arrays on Orbital Angular Momentum (OAM) Modes," in 2022 14th German Microwave Conference (GeMiC), pp. 164–167, Ulm, Germany, 2022.
[22] Y. Zhao, Z.Wang, Y. Lu, and Y. L. Guan, "Multi-mode OAM Convergent Transmission with Co-divergent Angle Tailored by Airy Wavefront," IEEE Transactions on Antennas and Propagation, vol. 71, pp. 5256– 5265, Jun. 2023.
[23] T. Yuan, H. Wang, Y. Qin, and Y. Cheng, "Electromagnetic Vortex Imaging Using Uniform Concentric Circular Arrays," IEEE Antennas and Wireless Propagation Letters, vol. 15, pp. 1024–1027, Oct. 2016.
[24] M. Wulff, L. Wang, C. Yang, H. D. Brüns, and C. Schuster, "Using Orbital Angular Momentum (OAM) Modes on Multi-Conductor Cables for Crosstalk Mitigation," in 2020 IEEE 24th Workshop on Signal and Power Integrity (SPI), Cologne, Germany, 2020.
[25] M. Wulff, T. Hillebrecht, L. Wang, C. Yang, and C. Schuster, "Multiconductor Transmission Lines for Orbital Angular Momentum (OAM) Communication Links," IEEE Transactions on Components, Packaging and Manufacturing Technology, vol. 12, pp. 329–340, Feb. 2022.
[26] M. Wulff, L. Wang, C. Yang, and C. Schuster, "Inter Mode Interference in Circular Antenna Arrays for Orbital Angular Momentum (OAM) Based Communication," in 2022 IEEE International Symposium on Antennas and Propagation and USNC-URSI Radio Science Meeting (AP-S/URSI), pp. 1976–1977, Denver, CO, USA, 2022.
[27] M. Wulff, L. Wang, A. Kölpin, and C. Schuster, "Influence of the Communication Environment on Orbital Angular Momentum (OAM) Mode Orthogonality," in 2023 52nd European Microwave Conference (EuMC), Berlin, Germany, 2023.
[28] M. Najafi, Einfluss von Elementausrichtung und –typus auf ein Orbital Angular Momentum (OAM) Antennen-Array . Bachelor's thesis, Hamburg University of Technology (TUHH), Hamburg, Germany, 2021.
[29] L. Wang, F. Jiang, M. Chen, H. Dou, G. Gui, and H. Sari, "Interference Mitigation Based on Optimal Modes Selection Strategy and CMAMIMO Equalization for OAM-MIMO Communications," IEEE Access, vol. 6, pp. 69850–69859, 2018.
[30] M. Wulff, Numerical Analysis of Orbital Angular Momentum Waves Regarding Wave Propagation and Communication. Dissertation, Hamburg University of Technology (TUHH), Hamburg, Germany, 2023 (submitted).
[31] M. Gehm, Influence of Interfering Antennas on Orbital Angular Momentum (OAM) Communication. Bachelor's thesis, Hamburg University of Technology (TUHH), Hamburg, Germany, 2023.
[32] M. Wulff, L. Wang, H.-D. Brüns, and C. Schuster, "Simulating Aperture Coupling of OAM Waves Through an Infinite PEC Plane Using EFIE- MoM—Part II: Application and Interpretation," IEEE Transactions on Electromagnetic Compatibility, vol. 65, pp. 1400–1409, July 2023.
[33] M. Wulff, T. Zhang, L. Wang, H.-D. Brüns, and C. Schuster, "Simulating Aperture Coupling of OAM Waves Through an Infinite PEC Plane Using EFIE-MoM—Part I: Validation and Numerical Accuracy," IEEE Transactions on Electromagnetic Compatibility, vol. 65, pp. 1389–1399, July 2023.
[34] M. Wulff, W. Park, L. Wang, C. Yang, H.-D. Brüns, and C. Schuster, "Shielding of Orbital Angular Momentum Waves by a Cavity With Apertures," IEEE Transactions on Electromagnetic Compatibility, vol. 64, pp. 692–701, June

Biographies

Michael Wulff received the B.Sc. and M.Sc. degree in electrical engineering from the Hamburg University of Technology, Hamburg, Germany, in 2017 and 2019, respectively, were he is currently pursuing the Ph.D. degree with the Institute of Electromagnetic Theory. His current research interests include the analysis of orbital angular momentum-based communication.

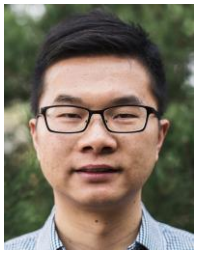

Lei Wang received the Ph.D. degree in electromagnetic field and microwave technology from the Southeast University, Nanjing, China in 2015. From 2014 to 2016, he was a Research Fellow and Postdoc in the Laboratory of Electromagnetics and Antennas, Swiss Federal Institute of Technology (EPFL) in Lausanne, Switzerland. From 2016 to 2017, he was a Postdoc in Electromagnetic Engineering Laboratory of KTH Royal Institute of Technology in Stockholm, Sweden. From 2017 to 2020, he was an Alexander von Humboldt fellow in the Institute of Electromagnetic Theory of Hamburg University of Technology in Hamburg, Germany. From 2020 to 2024, he was an Assistant Professor in the Institute of Signals, Sensors and Systems of Heriot-Watt University in Edinburgh, United Kingdom. From 2024, he is a Senior Lecturer in the School of Engineering at the Lancaster University in Lancaster, United Kingdom. His research includes the antenna theory and applications, active electronically scanning arrays, integrated antennas and arrays, substrate-integrated waveguide antennas, leaky-wave antennas, wireless power transfer, and wireless propagations.

He has published more than 80 peer-review papers, book chapters, in addition to UK&US patents. He is the awardee of the National PhD Scholarship in China (2014), the Swiss Government Excellence Scholarship (2014), the Alexander von Humboldt fellowship (2016), Principal Investigator grant from German Research Foundation (DFG) (2020), the British Royal Society research grant (2022), the UK EPSRC international collaboration grant (2023). Moreover, he received the Best Poster Award in iWAT-2018, the Best Paper Award in UCET-2020, and the Best Theory and Design Antenna Paper Award in EuCAP-2023. He also supervised students winning the Honourable Mentioned Best Student Paper Award in APS-2021, the Best Student Paper Award in UCMMT-2022, the Second Place Winner in IWS-2023, and school postgraduate research prizes (2022, 2023).

Christian Schuster received the Diploma degree in physics from the University of Konstanz, Germany, in 1996, and the Ph. D. degree in electrical engineering from the Swiss Federal Institute of Technology (ETH), Zurich, Switzerland, in 2000. Since 2006 he is full professor and head of the Institute of Electromagnetic Theory at the Hamburg University of Technology (TUHH), Germany. Prior to that he was with the IBM T. J. Watson Research Center, Yorktown Heights, NY, where he was involved in high-speed optoelectronic package and backplane interconnect modeling and signal integrity design for new server generations. His currents interests include signal and power integrity of digital systems, multiport measurement and calibration techniques, and development of electromagnetic simulation methods for communication electronics.

Dr. Schuster received IEEE Transactions on EMC Paper Awards in 2002 and 2015, IEEE Transactions on CPMT Paper Awards in 2012 and 2016, DesignCon Paper Awards in 2006, 2010, 2017 and 2018, three IBM Research Division Awards between 2003 and 2005, and IBM Faculty Awards in 2009 and 2010. Also, in 2019 he received the Sustained Service to the EMC Society Award. He is a member of the German Physical Society (DPG) and several technical program committees of international conferences on signal and power integrity, and electromagnetic compatibility. He was serving as a Distinguished Lecturer for the IEEE EMC Society in the period 2012-2013, as the Chair of the German IEEE EMC Chapter in the period 2016-2019, as a member of the Board of Directors of the EMC Society in 2015 and in the period 2020-2022, and is currently an Associate Editor for the IEEE Transactions on EMC as well as an Adjunct Associate Professor at the School of Electrical and Computer Engineering of the Georgia Institute of Technology.